Article

Reversible Trilayer Formation at the Air–Water Interface from a Mixed Monolayer Containing a Cationic Lipid and an Anionic Porphyrin

Marta Prez-Morales, Jos M. Pedrosa, Mara T. Martn-Romero, Dietmar Mbius, and Luis Camacho

J. Phys. Chem. B, **2004**, 108 (14), 4457-4465• DOI: 10.1021/jp037282k • Publication Date (Web): 16 March 2004

Reversible Trilayer Formation at the Air−Water Interface from a Mixed Monolayer Containing a Cationic Lipid and an Anionic Porphyrin

Marta Pérez-Morales,[†] José M. Pedrosa,[‡] María T. Martín-Romero,*[,†] Dietmar Möbius,[§] and Luis Camacho*[,†]

Departamento de Química Física y Termodinámica Aplicada, Universidad de Córdoba, Campus Universitario de Rabanales, Ed. Marie Curie, E-14071 Córdoba, Spain, Departamento de Ciencias Ambientales, Universidad Pablo de Olavide, Crta. Utrera km 1, E-41013 Sevilla, Spain, and Max-Planck-Institut für biophysikalische Chemie (Abt. Nanobiophotonik), D-37077 Göttingen, Germany

Received: October 30, 2003; In Final Form: February 10, 2004

The molecular organization of a cationic matrix (DOMA) as influenced by the presence of an anionic water-soluble porphyrin (TSPP), in the mixed monolayer, molar ratio TSPP/DOMA = 1:4, has been studied by $\pi-A$ isotherms, the reflection spectra, BAM images, and imaging ellipsometry at the air−water interface. A reversible collapse of the mixed film at high surface pressures is observed. The formation of an aggregate of the porphyrin molecules under compression is inferred from the reflection spectra. BAM images show the spontaneous formation of domains at 35 mN/m that become bigger during the spontaneous dense process at constant surface pressure. The reversible character of that process was also observed by BAM. The evaluation of the reflection spectra as well as the area fraction of the domains and the surrounding dark regions have led us to consider a trilayer structure for the TSPP/DOMA domains emerging during the collapse process. By using imaging ellipsometry on selected regions of interest (few microns), the thicknesses of domains (d_{dom} = 5.045 nm) and surrounding areas (d_{dark} = 1.764 nm) were estimated. These thickness values are in good agreement with the trilayer architecture where the DOMA molecules have retained the TSPP molecules by electrostatic interactions.

Introduction

The development of novel functionalized materials and the use of new principles of device functioning have led the study of organic ultrathin films. The biomimetic approach may provide new insight into the design, development, assembly, and functionalization of new materials and systems at the molecular level. The physical principles which drive the interactions leading to the formation of self-assembled and self-organized molecular and nanoscopic systems have been widely investigated over the last years to establish a relationship between chemical composition, structure, and organization of these materials and systems with the desired physical properties and functions.[1]

The environment and orientation of functional molecules may be controlled by incorporation in molecular assemblies. Assembling and handling organized ultrathin films containing different molecules with various functions and well-defined architecture (composition, structure, and thickness) is a promising method for constructing molecular devices.[2] In this sense, a large research effort has been directed to the design of arranged surfaces that are able to control the orientation at the molecular level in a reproducible way, e.g. in devices designed for high resolution. The air−water interface is an ideal model surface for this purpose because it is easy to prepare in a pure state and because the surface coverage can be smoothly adjusted by using the Langmuir trough technique. A monolayer or multilayer at this interface can be used as a well-defined model to study interactions within layers.

Although there have been major advances in our understanding of phase transitions in Langmuir monolayers during the past decade,[1] the process of collapse, the transition of a monolayer to a three-dimensional phase, by which floating material is forced out of the monolayer at high compression to form multilayer or bulk structures, needs further investigation. In particular, the collapse of monolayers of liquid-crystalline phases is of special interest due to the intrinsic long-range orientational order that these systems possess. In some cases, the collapse process has been viewed as the folding up and sliding of molecular layers on top of one another.[3,4] For example, Xue et al.[5] studied the collapse of a monolayer of a thermotropic liquid crystal that was consistent with a model in which the monolayer "collapses" through a transition to a homogeneous trilayer film composed of a monolayer plus an interdigitated bilayer. This collapse can form monolayers and multilayers at the air−water interface with a high degree of order compared to other monolayer systems as demonstrated by de Mul and Mann.[6] Also, the plateau observed in the $\pi-A$ isotherms of aromatic carboxylic acids[7] revealed a similar behavior to that observed for mesogenic substances.[3−5] Recently, Gourier et al.[8] have obtained evidence for the folding and displacement of one portion of the pentacosadiyonic acid monolayer with respect to another (sliding mechanism for collapse). By the collapse phase detected during the surface pressure−area isotherm at the air−water interface, Huo et al.[9] demonstrated the formation of a

* To whom correspondence should be addressed. E-mail: qf1cadel@uco.es.
[†] Departamento de Química Física, Universidad de Córdoba.
[‡] Departamento de Ciencias Ambientales, Universidad Pablo de Olavide.
[§] Max-Planck-Institut für biophysikalische Chemie.

10.1021/jp037282k CCC: $27.50
Published on Web 03/16/2004

SCHEME 1. Molecular Structures of DOMA and TSPP

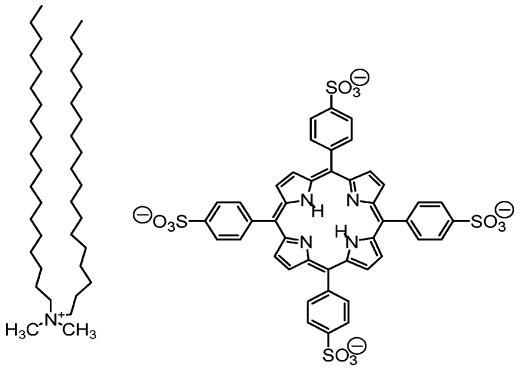

bilayer in a new nontraditional supramolecular-like Langmuir film with a urea derivative.

A great number of experimental approaches have been utilized to study the mechanism of monolayer collapse. Thus, the confirmation of the structure along the "collapse" process in Langmuir monolayers may be given with techniques noninvasive such as BAM (Brewster angle microscopy)[10,11] and ellipsometry of the film on the interface.[4,7,12,13] Some of the earliest investigations of the mechanisms of collapse were performed by Ries,[14] who prepared Langmuir−Blodgett films collapsing monolayers and imaged them by electron microscopy. More recently, several groups have carried out similar experiments in which the topography of collapsed films of fatty acids was determined by AFM.[15−19] Also, GIXD and reflectivity studies of collapsed films of cholesterol have indicated a model in which there is a mixture of monolayers, a smooth bilayer, and a crystalline trilayer covered by a disordered monolayer.[20]

In the present work, the molecular organization of a mixed film containing a cationic matrix (DOMA) and a tetraanionic water-soluble porphyrin (TSPP) at the air−water interface has been investigated. The results obtained by means of surface techniques, such as reflection spectroscopy, BAM, and ellipsometry, lead to a nontraditional collapse where a novel, stable, and reversible superstructure of the TSPP/DOMA, ratio 1:4, is formed at the air−water interface. The organization of the mixed ultrathin film spontaneously formed at high surface pressure corresponds to a trilayer film, where a bilayer of DOMA molecules whose head polar groups retain the dimer porphyrins stands on top of a mixed monolayer with monomer porphyrins.

Experimental Section

Materials. Dioctadecyldimethylammonium bromide (DOMA) was purchased from Sigma Chemical Co. and used as received. Tetrakis(4-sulfonatophenyl)porphyrin (TSPP) was supplied by Fluka and used without purification. Their molecular structures are depicted in Scheme 1. A mixture of dichloromethane, methanol, and water, ratio 15:9:2 (v/v/v), was used as spreading solvent for solving both components. The pure solvents were obtained without further purification from Panreac (Spain) and Baker Chemicals (Germany). The water for the subphase and for the mixture spreading solvent was prepared with a Millipore Mill-Q unit, pretreated by a Millipore Reverse Osmosis system (>18 M$\Omega\cdot$cm^{-1}).

Preparation of the Mixed Monolayers at the Air−Water Interface. Mixed monolayers of TSPP/DOMA, in a molar ratio of 1:4, were prepared by cospreading (the mixed solution of the two components)[21−24] onto a pure water subphase at 21 °C on a Nima Langmuir trough provided with a Wilhelmy-type dynamometric system using a plate of filter paper for good wettability. This device was used for all measurements done on the mixed film, i.e., surface pressure−area ($\pi-A$) isotherms, characterization of the stability of the monolayers, reflection spectroscopy at normal incidence, visualization by Brewster angle microscopy (BAM), and ellipsometry. After cospreading of the mixed solution on the water surface, 15 min were left for evaporation of the solvent and the monolayers were compressed at a speed of $\sim$0.1 nm^2 min^{-1} molecule^{-1}.

Reflection Spectroscopy. The difference in reflectivity, ΔR, of the monolayer-covered water surface and the bare water surface is determined. Details of the reflection spectrometer have been described elsewhere.[25]

Ellipsometric Measurements. Ellipsometric measurements were performed with a PCSA null imaging ellipsometer (I-Elli2000 supplied by NFT, Nanofilm Technologie, Göttingen, Germany) using a solid-state laser (wavelength 532 nm, 50 mW). The accuracy of the device is 0.02° in Δ and Ψ. For measurements of the films at the air−water interface we used an angle of incidence (ϕ) of 50°. The ellipsometric angles, Δ and Ψ, were measured on different regions of interest (ROI, minimum size of about 20 μm) avoiding any lateral structure or defect within the spot size of the beam and resulting in valuable results and keeping spatial information. The average from 20 experimental measurements has been used. The calculations were performed according to ellipsometric equations (see the Appendix).[26] The Δ and Ψ values are related to the ratio of the Fresnel reflection coefficients by $R_p/R_s = \tan(\Psi)\exp(i\Delta)$, where R_p and R_s are the parallel and normal components, respectively, with respect to the plane of incidence of electric vector E.

The I-Elli2000 is also equipped with an imaging device by which images of the film at the Brewster angle (Brewster angle microscopy, BAM) can be recorded with a lateral resolution of 2 μm. The image processing procedure included a geometrical correction of the image, as well as a filtering operation to reduce interference fringes and noise. Furthermore, the brightness of each image was scaled to improve contrast. The microscope and the film balance were located on a table with vibration isolation (anti-vibration system MOD-2 S, Halcyonics, Göttingen, Germany) in a large class 100 clean room.

Results

Surface Pressure−Area Isotherms. Monolayers of TSPP/DOMA, in a molar ratio of 1:4, were formed at the air−water interface. This mixing ratio corresponds to the stoichiometry forming neutral monolayers and thus we expect that all molecules of porphyrin remain bound to the lipid matrix by electrostatic interactions, although it must be tested experimentally.

Figure 1 (top) shows the $\pi-A$ isotherms of DOMA (dashed line) and TSPP/DOMA = 1:4 (solid line). Both isotherms are expressed per DOMA molecule, therefore any expansion with respect to the pure lipid isotherm is a clear evidence for the presence of the porphyrin molecules at the interface. Effectively, an expansion from low surface pressure up to 35 mN/m is observed.

The most noticeable phenomena observed along the isotherm of the mixed monolayer (solid line) are the surface pressure drop as the mixed film is compressed at $A < 0.75$ nm^2 and the subsequent decrease of the DOMA area from approximately 0.75 nm^2 to 0.28 nm^2 (at $\pi = 38$ mN/m) in contrast with the constant molecular area of DOMA at $\pi \approx 38$ mN/m, $A \approx 0.50$ nm^2, measured for the isotherm of the pure lipid in the absence

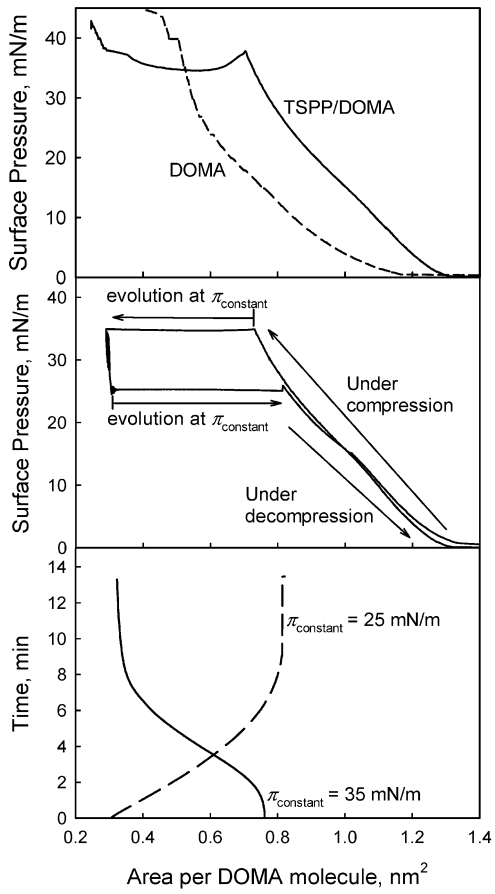

Figure 1. Top: Surface pressure−area isotherms of DOMA (dashed line) and TSPP/DOMA = 1:4 (solid line) at the air−water interface. Middle: Cyclic isotherm of the mixed monolayer as follows, under compression from 0 to 35 mN/m, evolution at $\pi_{constant}$ = 35 mN/m, decompression to 25 mN/m, evolution at $\pi_{constant}$ = 25 mN/m, and decompression from 25 to 0 mN/m. Bottom: Time−area curves obtained at $\pi_{constant}$ = 35 mN/m (solid line) and $\pi_{constant}$ = 25 mN/m (dashed line).

of porphyrin. Both phenomena should be taken as indicating collapse, i.e., expulsion of molecules from the film to form a new phase.[27] However, this collapse is not strictly speaking a "traditional collapse" since as described below the new phase forms a well-defined and stable multilayer film.

The isotherm of the TSPP/DOMA = 1:4 system obtained here differs meaningfully from that measured by Zhang et al. spreading DOMA on the aqueous subphase containing TSPP.[28] Those authors detected the adsorption of the TSPP molecules from the subphase to the lipid matrix without observing the collapse registered for our mixed monolayer prepared by the cospreading method.

To study the stability of the mixed monolayer at the air−water interface, as well as the nature of the observed collapse at high surface pressures, successive cycles of compression (up to 40 mN·m^{-1}) and expansion of the film were recorded, and no hysteresis was detected (data not shown).

The stability of the mixed film was also studied at constant surface pressure. The film was compressed to a fixed surface pressure, $\pi_{constant}$ (Figure 1, middle), and the spontaneous evolution of the monolayer at that $\pi_{constant}$ was registered as $t-A$ curves (Figure 1, bottom). The area relaxation was dependent on the surface pressure, $\pi_{constant}$, chosen. Thus, at $\pi_{constant} < 33.5$ mN/m the loss of area was negligible after 1 h. However, at $\pi_{constant} \geq 33.5$ mN/m a spontaneous condensation process of the mixed monolayer was registered. Further, at

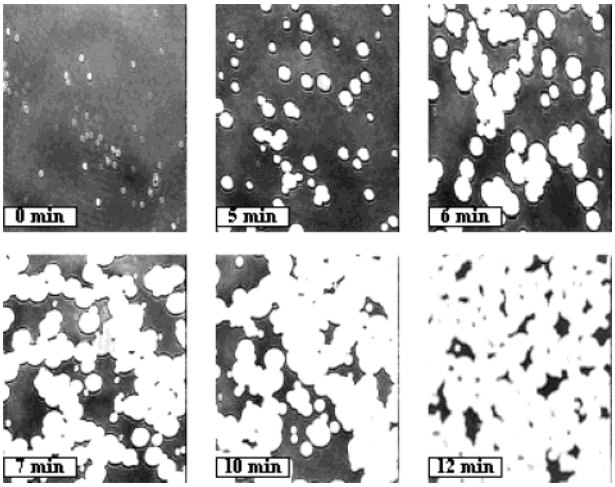

Figure 2. Growing of the bright domains observed by BAM of the mixed TSPP/DOMA monolayer under constant surface pressure of 35 mN/m. Image size: 430 μm width.

$\pi_{constant}$ slightly higher than 33.5 mN/m the relaxation process is very slow, while at $\pi_{constant} > 38$ mN/m the process occurs in a few seconds. Figure 1 (middle and bottom) shows the measurement at $\pi_{constant}$ = 35 mN/m. At that point, the area diminished to a constant value of 0.32 nm^2 per DOMA molecule (∼12 min), where the monolayer was stable for a long period of time. The area reached depends slightly on the selected $\pi_{constant}$ value.

Once the equilibrium state was reached, the film was expanded at different surface pressures and then the evolution of area at $\pi_{constant}$ was recorded (at 25 mN/m in Figure 1, middle and bottom). A spontaneous expansion stabilizing at A = 0.83 nm^2 (value previously reached under compression at 25 mN/m) was observed. The rate of this process also depends on the $\pi_{constant}$ chosen. At this point of the experiment, the $\pi-A$ isotherm to low surface pressure was registered under decompression and no hysteresis was observed.

This type of measurement demonstrated not only the stability of the mixed monolayer, but also that the pressure drop at $\pi >$ 38 mN/m was due to a kinetic effect that originated from the compression rate of the film. Under equilibrium conditions, the pressure drop does not occur. Further, although the area decrease of the mixed monolayer with respect to that of the lipid film points out collapse, such a collapse seems to lead the film to a well-defined and stable multilayer film.

BAM Images. Simultaneous to the measurement described in Figure 1 (bottom), the morphology of the mixed TSPP/DOMA = 1:4 monolayer at the air−water interface was directly observed by BAM (Figure 2). Initially, the mixed monolayer appears homogeneous (images not shown). However, when an area of $A \approx 0.75$ nm^2/DOMA (at 35 mN/m) molecule is reached upon compression some small bright domains form on a slightly darker surrounding area (Figure 2, 0 min). Keeping the surface pressure constant, $\pi_{constant}$ = 35 mN/m, those bright domains grow spontaneously filling almost the whole field of view in a few minutes (sequence of images in Figure 2). During this phenomenon, the film area decreases from $A \approx 0.75$ (t = 0 min) to 0.32 nm^2 ($t \approx 12$ min) as shown in Figure 1 (bottom). For A = 0.32 nm^2/DOMA, the bright domains fill about 79% of the surface area while an area fraction of 0.21 is occupied by the dark regions.

Imaging Ellipsometry. Ellipsometry was established long ago as a sensitive method for obtaining data about surfaces and thin films.[29,30] Reliable estimations of thicknesses of polymer

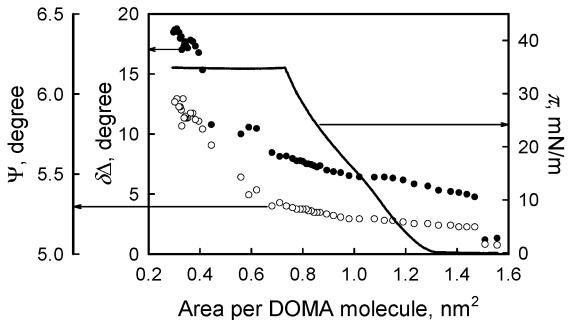

Figure 3. Elli-isotherms of the mixed TSPP/DOMA film at the air−water interface: $\delta\Delta$ versus A (full circles) and Ψ versus A (open circles). $\pi-A$ (solid line) is shown as a reference. The values of $\delta\Delta$ and Ψ were measured overall spot light (430 μm × 530 μm).

films can be obtained from ellipsometric data (Δ, Ψ). However, the ellipsometric information may be incomplete, and a careful analysis is needed to obtain the structural information of the films.[31]

Figure 3 shows the change of the ellipsometric angles $\delta\Delta$ ($\delta\Delta = \Delta - \Delta_0$, where Δ is obtained in the presence of a film and Δ_0 in the absence of a film, i.e., water surface) and Ψ versus area ($\delta\Delta-A$ and $\Psi-A$ isotherms) during the compression of the TSPP/DOMA = 1:4 monolayer. The $\delta\Delta$ and Ψ values plotted in this figure correspond to the average on a large region of the film (430 μm × 530 μm, spot of laser). The $\pi-A$ isotherm of the mixed monolayer is also shown as a reference.

Conventional approaches of ellipsometry involve averaging the signal over the entire diameter of the light beam (usually a laser). As a consequence, all spatial information of the film, being homogeneous or not, and including defects such as scratches, dust, etc., is reduced into a single number for each of the ellipsometric quantities Δ and Ψ, leaving the real structure up to anyone's guess. The imaging ellipsometry technique employed here has allowed us for the first time to measure the ellipsometric angles in selected, homogeneous regions (ROI, region of interest) with a size of just a few microns (~20 μm × 20 μm) at the air−water interface. Therefore various values of the ellipsometric angles, Δ and Ψ, for the different regions observed at that interface, i.e., domains and surrounding areas, can be obtained.

Upon compression up to 35 mN/m and during the spontaneous condensed process of the mixed film decreasing its area to 0.32 nm^2 (Figure 1, middle), different values of $\delta\Delta$ and Ψ as a function of the ROI location were obtained. When the ROI is located upon the dark regions (see Figure 2), $\delta\Delta_{dark} = 7.5 \pm 0.1°$ and $\Psi_{dark} = 5.22 \pm 0.05°$. These $\delta\Delta$ and Ψ experimental values are constant during the whole relaxation process and they are coincident with those obtained for $A = 0.75$ nm^2 (see Figure 3). It must be pointed out that this coincidence is only possible where the structure and composition of the films is identical. Therefore, the area per DOMA molecule in the dark regions must be $A_{dark} \approx 0.75$ nm^2.

The ellipsometric angles, Δ and Ψ, also were measured on the bright domains (see Figure 2). Different regions of the image were studied by using ROI of different sizes and the averages obtained were $\delta\Delta_{dom} = 18.3 \pm 0.1°$ and $\Psi_{dom} = 5.93 \pm 0.05°$. These $\delta\Delta$ and Ψ experimental values are practically constant through the whole relaxation process.

The fact that the optical properties ($\delta\Delta$ and Ψ) of domains and dark regions remain constant throughout the condensation (relaxation) process is evidence of a phase transition between two organized phases.

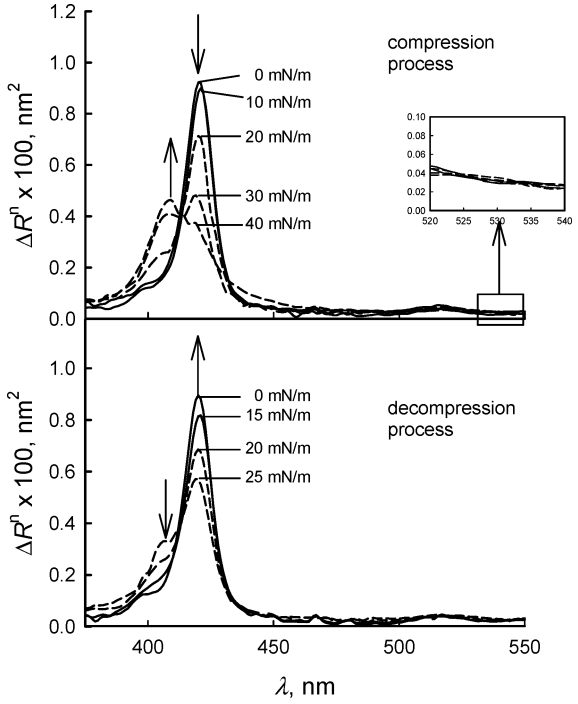

Figure 4. Reflection spectra normalized at the same surface density of DOMA, ΔR^n, under compression (top: 0 ($A = 1.38$ nm^2), 10 ($A = 1.14$ nm^2), 20 ($A = 0.95$ nm^2), 30 ($A = 0.80$ nm^2), and 40 mN/m ($A = 0.26$ nm^2)) and decompression (bottom: 25 ($A = 0.26$ nm^2), 20 ($A = 0.94$ nm^2), 15 ($A = 1.04$ nm^2), and 0 mN/m ($A = 1.36$ nm^2)). The inset shows the expansion of those spectra during the compression process in the wavelength range of 520−540 nm. Solid lines are for those spectra with only $\lambda_{max} = 420$ nm, and dashed lines are for those with a new band at 408 nm.

Reflection Measurements. To detect directly the presence of the porphyrin molecules in the mixed monolayer with DOMA, a series of reflection spectra at different surface pressures were measured during the compression and decompression processes. This technique gives us valuable information on the organization, density, and orientation of the chomophore molecules located at the air−water interface.

In Figure 4, the normalized reflection spectra ($\Delta R^n = \Delta R \times A$) obtained for TSPP/DOMA, molar ratio 1:4, at different surface pressures during the compression (top) and expansion (bottom) processes at the air−water interface are shown. These spectra consist of an intense Soret band and small Q-bands, typical for a porphyrin. Two remarkable phenomena are observed in these spectra: first, the decreasing of the Soret band with maximum at 420 nm, close to that measured in organic solution ($\lambda_{max} = 416$ nm), and the appearance of a new band at 408 nm as the surface density of porphyrin increases ($\Delta\lambda = -12$ nm); and second, the recovery of the system during the expansion process as recorded in the reflection spectra. The coincidence of those spectra during the compression and expansion processes recorded at low surface pressure (0 mN/m) is experimental evidence that there is no appreciable loss of porphyrin molecules into the aqueous subphase.

Discussion

The experimental data obtained by reflection spectroscopy, a shift to shorter wavelengths by ~10 nm, with respect to the maximum wavelength at low surface pressure, have been observed for similar mixed systems of M-TMPyP/DMPA (cationic porphyrins, Ni(II)-tetrakis(4-methylpyridyl)porphyrin, and H_2-tetrakis(4-methylpyridyl)porphine, M-TMPyP, M = H_2,

SCHEME 2. Stacked Dimer of the TSPP Molecules

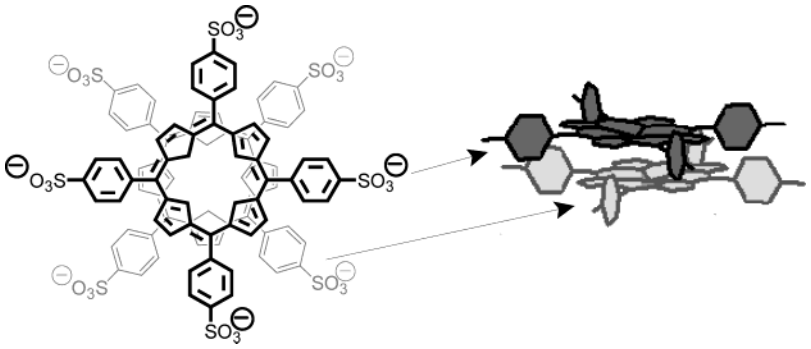

Ni(II), and a lipid with negatively charged headgroups, L-α-dimyristoylphosphatidic acid, DMPA), where a dimer−monomer equilibrium was described.[21,22] In such cases, the blue shift was assigned to a stacked dimer formation (H aggregate) with the porphyrin rings lying parallel and twisted by 45° with respect to each other underneath the phospholipid matrix (all porphyrin molecules have access to phospholipid headgroups).

Assuming that configuration for the TSPP/DOMA system, and applying the extended dipole model[32] with a thickness of TSPP $r = 3.5$ Å, a dielectric constant of $D = 2.67$, and an oscillator strength $f = 2.08$ (calculated in organic solution), the values calculated for the dipole length and charge are $l = 8.70$ Å and $q = 0.208e$, respectively, for $\Delta\lambda = -12$ nm. These values are in very good agreement with respect to those obtained for similar systems.[22] Thus, $\lambda_{max} = 420$ nm is assigned to the monomer porphyrin, while $\lambda_{max} = 408$ nm is assigned to the stacked dimer of TSPP molecules (see Scheme 2).

For low values of absorption, the reflection ΔR, is given in a reasonable approximation by[25]

$$\Delta R = (2.303 \times 10^3)\Gamma f_{orient}\epsilon\sqrt{R_s} \qquad (1)$$

where Γ is the surface concentration in mol cm^{-2}, $R_s = 0.02$[33] is the reflectivity of the interface air−water at normal incidence, ϵ is the extinction coefficient given as L mol^{-1} cm^{-1}, and f_{orient} is a numerical factor that takes into account the different average orientation of the porphyrin chromophore in solution as compared to the monolayer at the air−water interface. For a general case, the orientation factor is given by

$$f_{orient} = {}^3/_4[1 + \langle \sin\theta \rangle^2] \qquad (2)$$

with θ being the angle between the plane of the transition moments and the normal to the air−water interface (angle brackets denote average values).[34] In this mixed system, at low surface pressures $\Delta R^n(0\ \text{mN m}^{-1})_{compression} \approx \Delta R^n(0\ \text{mN m}^{-1})_{expansion} \approx 0.92$ (see Figure 4). This value is in very good agreement with that obtained from eq 1 ($\Delta R^n \approx 0.90$) and assuming $\epsilon = \epsilon_{solution}$ at λ_{max} ($\epsilon_{solution,420} = 4.5 \times 10^5$ L mol^{-1} cm^{-1}), flat orientation ($f_{orient} = 1.5$), and no loss of TSPP molecules. However, during the whole compression process a further analysis has to be done as follows.

From the measured reflection spectra an apparent oscillator strength is defined as[35,36]

$$f_{app} = f \times f_{orient} = (2.6 \times 10^{-12})\int_{band} A\Delta R\, d\upsilon = (2.6 \times 10^{-12})\int_{band} \Delta R^n\, d\upsilon \qquad (3)$$

where f is the oscillator strength in solution, A is the area per molecule, υ is the frequency, and the numeric factor 2.6×10^{-12} is expressed in nm^{-2} s. Thus, f_{app} is obtained by the integration of the reflection band in the range between 370 and 475 nm. The values of f_{app} evaluated from three series of reflection spectra of the mixed monolayer at the air−water interface are plotted against the area per DOMA molecule in Figure 5.

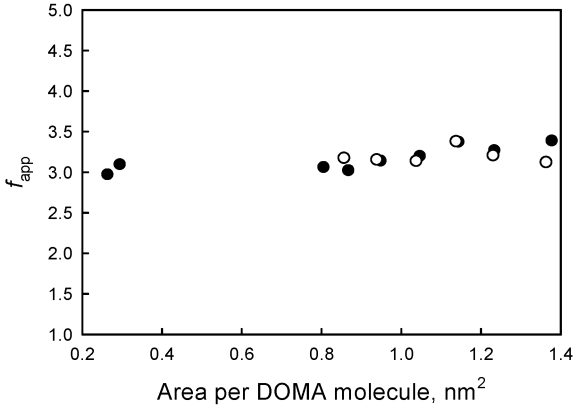

Figure 5. Plot of the apparent oscillator strength f_{app} determined according to eq 3 and with the reflection spectra obtained during the compression (full circles) and decompression (empty circles) processes, against area per DOMA molecule.

Two effects are clearly visible in this figure: (1) the value of f_{app} is almost constant at any surface density and (2) there is a good coincidence between the f_{app} values during compression (full circles) and subsequent decompression (empty circles) processes. Moreover, the ratio between this apparent oscillator strength, $f_{app} = 3.13$, and the oscillator strength obtained from the solution spectrum, $f = 2.08$, gives by eq 3 $f_{orient} = 1.5$ for any surface pressure. This is the maximum value that can be obtained only if there is no loss of the porphyrin molecules into the aqueous subphase and if those molecules lie parallel to the interface ($\theta = 90°$ by eq 2). This is unambiguous evidence both for a flat orientation of the porphyrin rings at any surface pressure and for the presence of all molecules of porphyrin cospread at the interface.

The dimer formation at the air−water interface and the flat orientation of the porphyrin molecules at any surface area allow us to consider a dimer−monomer equilibrium for TSPP similar to that proposed in previous works for other water-soluble porphyrins (M-TMPyP) where all porphyrin molecules have access to the charges of the phospholipid matrix.

To prove that molecular model, the monomer (sf_{mon}) and dimer ($1 - sf_{mon}$) surface fractions at different surface pressures have been determined from the reflection spectra considering that for intermediate surface pressures, the normalized reflection spectra can be evaluated by the equation

$$\Delta R^n = sf_{mon}\Delta R^n_{mon} + (1 - sf_{mon})\Delta R^n_{dim} \qquad (4)$$

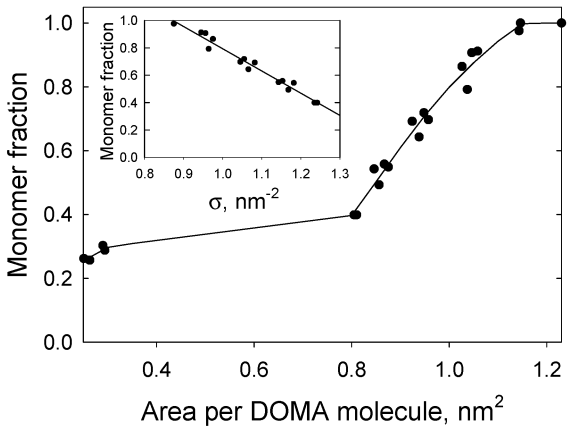

Figure 6. Variation of monomer fraction versus area per DOMA molecule. Inset: Plot of monomer fraction vs density.

where ΔR^{n}_{mon} is known and corresponds to that registered at 0 mN/m (see Figure 4, top). The sf_{mon} values have been obtained by numerical adjustment to eq 4 under the condition that the normalized reflection spectrum of the dimer, ΔR^{n}_{dim}, should be the same for each analyzed spectrum (good agreement between those spectra has been obtained during the adjustment process). In Figure 6, the sf_{mon} values are plotted versus area per DOMA molecule in the mixed monolayer. The monomer fraction starts to decrease for $A \approx 1.15$ nm^2/DOMA, being $sf_{mon} \approx 0.4$ for $A \approx 0.8$ nm^2/DOMA. Supposing the dimer−monomer equilibrium, the surface density ($\sigma = A^{-1}$) of the DOMA will be

$$\sigma = sf_{mon}\sigma_{mon} + (1 - sf_{mon})\sigma_{dim} \qquad (5)$$

where σ_{mon} and σ_{dim} correspond to the molecular density per DOMA molecule in the different regions in which the TSPP molecules are monomer and dimer, respectively.

The plot of sf_{mon} versus σ (inset Figure 6) allows us to determine $A_{mon} = \sigma_{mon}{}^{-1} = 1.14$ nm^2/DOMA and $A_{dim} = \sigma_{dim}{}^{-1} = 0.67$ nm^2/DOMA, which correspond to the DOMA area for $TSPP_{monomer}$−DOMA and $TSPP_{dimer}$−DOMA complexes, respectively.

Inasmuch as the molar ratio of TSPP/DOMA is 1:4, the area per $TSPP_{monomer}$−DOMA (TSPP + 4 DOMA) will be $4 \times A_{mon} = 4.56$ nm^2. This value is slightly higher than that of the flat TSPP molecule (~3.20 nm^2).[24] This increase may be due to the organization of DOMA molecules compensating for the negative charges of the TSPP molecules which are spread partially on the TSPP area because of the headgroup size (ammonium group) and the orientation of the alkyl chains (they are not totally vertical with respect to the air−water interface). Therefore, the DOMA molecules contribute to the total area (4.56 nm^2) of the $TSPP_{monomer}$−DOMA complex (see Scheme 3).

On the other hand, the area per flat TSPP dimer should be similar to that of the monomer, ~3.20 nm^2 (see Scheme 2).[21] Now, 8 DOMA molecules must stay on top of the dimer compensating the 8 negative charges of the porphyrins. Thus, the area of the $TSPP_{dimer}$−DOMA complex will be $8 \times A_{dim} = 5.36$ nm^2. The $TSPP_{dimer}$−DOMA interaction requires all headgroups of DOMA molecules have access to the negative charges of the porphyrins, thus the DOMA molecules may stay at a different depth with respect to the interface as a function of the TSPP molecule that has to be compensated (see Scheme 3). Therefore, the lipid molecules have more contribution to the area complex for the $TSPP_{monomer}$−DOMA complex.

As commented before, the dimer−monomer equilibrium described for the TSPP/DOMA system from the reflection spectra is similar to that proposed for the M-TMPyP/DMPA,[21,22] at least regarding the porphyrin structure. However, analyzing the BAM images a noticeable difference can be appreciated. A substantial dimer fraction at $\pi = 30$ mN/m (see Figure 4) is detected by reflection measurements before the domains may be observed by BAM at 35 mN/m (see Figure 2 and comments), while the domains observed for the M-TMPyP/DMPA systems were demonstrated to be the dimer formation phase of the cationic porphyrin.[37]

For the M-TMPyP/DMPA systems, the areas of M-TMPyP monomer-4 DMPA and M-TMPyP dimer-8 DMPA agree to 3.2 nm^2 (value corresponding to the flat porphyrin area),[21] i.e., the phospholipid does not occupy additional area at the interface. However, the molecular structure of DOMA seems not to facilitate the coincidence of the two area complexes with that of the flat porphyrin. In turn, this fact could be related to the absence of domains from the $TSPP_{dimer}$-DOMA complex contrary to that observed for the M-TMPyP/DMPA system.[22,37] As depicted in Scheme 3, the TSPP dimers are laterally surrounded by the positive headgroups of DOMA molecules producing some electrostatic repulsions, and thus a random distribution of those complexes instead of an ordered one is produced. In such a case, the film stability decreases as the dimer complex densities increase ($A < 0.75$ nm^2), and consequently the collapse is generated and the domains can be visualized.

On the other hand, the small changes between the reflection spectra recorded before and after the collapse process (see Figure 4, at 30 mN/m before collapse, and 40 mN/m after collapse) seem to us a surprising feature of the collapse described. In fact, it was determined that the flat orientation of TSPP molecules with respect to the interface is conserved and the monomer fraction decreases slightly after the collapse process ($sf_{mon} \approx 0.4$ to 0.3, before to after collapse, respectively, see Figure 6).

The evaluation of the area fraction of the bright domains and the surrounding dark regions at high surface pressure from the BAM images may provide another approach to the architecture of this mixed system. Thus, for $A = 0.32$ nm^2/DOMA (Figure 2, $t = 12$ min), the bright domains fill about 79% of the surface area while an area fraction of 0.21 is occupied by the dark regions. If we assume different areas per DOMA molecule for the bright domains and the surrounding dark regions, and using $A = 0.75$ nm^2/DOMA for the area of the DOMA molecule at the dark regions, the area of DOMA for the bright domains, A_{dom}, can be determined from the following relationship of surface densities:

$$\frac{1}{0.32} = 0.79\frac{1}{A_{dom}} + 0.21\frac{1}{0.75} \qquad (6)$$

and an area per DOMA molecule in the domain of $A_{dom} = 0.28$ nm^2/DOMA is obtained. Since $A_{dom} = 0.28$ nm^2/DOMA is approximately equal to $^1/_3 \times 0.75$ nm^2/DOMA, the area per DOMA molecule in the bright domains is practically three times smaller than that measured in the dark surrounding regions, and therefore a trilayer structure for the TSPP/DOMA domains may be considered.

We propose that the mixed monolayer organizes at high surface pressure into a novel ordered trilayer film at the air−water interface (Scheme 4) where a bilayer of DOMA molecules whose head polar groups retain the dimer porphyrins stands on top of a mixed monolayer with monomer porphyrins. These trilayers correspond to the domains observed by BAM during

SCHEME 3. Model of the Possible Organization of the TSPP Molecules under the DOMA Matrix at the Air−Water Interface and under Compression below 33.5 mN/m

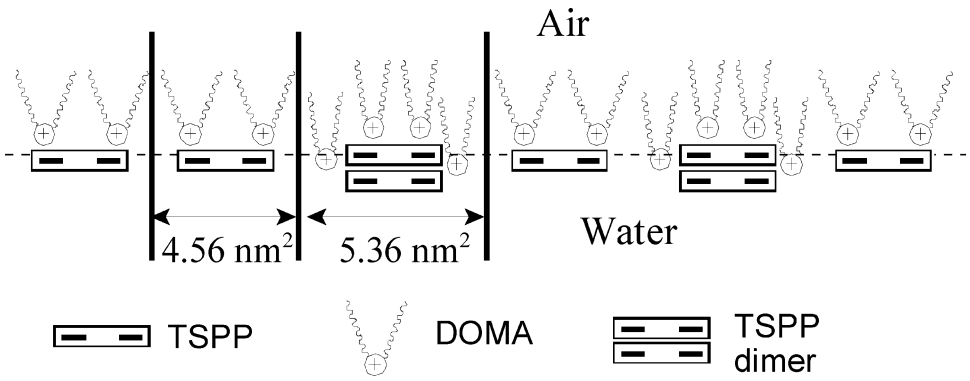

SCHEME 4. Model of the Trilayer Structure Formed during the Collapse Process at High Surface Pressures (π > 33.5 mN/m)

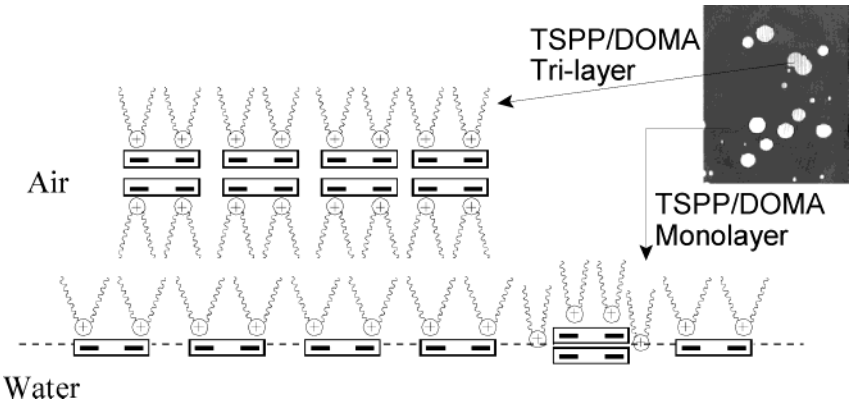

the collapse phenomenon. The experimental results obtained from the $\pi-A$ isotherm, the reflection spectroscopy, and BAM seem to confirm the proposed organization. In fact, according to that model the minimum fraction of monomer will be $^1/_3$, which almost agrees with that determined at high surface pressures where the whole surface is covered by domains.

To confirm the trilayer structure, a detailed analysis of the ellipsometric data has been done. The increase on the $\delta\Delta$ value for the bright domains ($\delta\Delta_{dom} = 18.3°$) with respect to that obtained from the dark regions ($\delta\Delta_{dark} = 7.5°$) must be mainly related to the increase of the film thickness. In the absence of absorption and considering a refractive index constant, $\delta\Delta$ must be proportional to the film thickness for thin films. The ratio $\delta\Delta_{dom}/\delta\Delta_{dark} = 2.44$ points out the strong increase of the film thickness, but it cannot be used to determine such an increase.[26]

When ellipsometric measurements are done at the air−water interface, laser beams where the monolayer does not absorb are frequently used. In those cases, only one experimental parameter, $\delta\Delta$, is meaningful since $\Psi_{film} = \Psi_{water}$. However, two unknown quantities, n and d, real parts of the refractive index and thickness, respectively, have to be determined, so the solution requires a previous knowledge of one of those unknown quantities. The presence of absorption (for our system, TSPP absorbs at 532 nm laser beam, see Figure 4) may seem an additional difficulty. However, it only involves a mathematical drawback. Now, the two experimental parameters, $\delta\Delta$ and Ψ, are meaningful and three quantities, n, d, and k (imaginary part of the refractive index), are unknown. As k may be estimated by a different method, the solution for n and d should be achieved.

A simultaneous calculation of the optical constants (n and k) and the thickness (d) from the Δ and Ψ values measured at only one wavelength and according to the ellipsometric equations[26] is not possible. However, the values of $\delta\Delta$ and Ψ contain valuable optical and structural information that can be extracted by means of transforming into the n, k, and d space. Such optical and structural information is given in Figure 7. The ellipsometric equations (see the Appendix) for d and k have been solved with the experimental $\delta\Delta$ and Ψ values and different n values. In such a way, if the experimental error of the measurements of $\delta\Delta$ and Ψ is excluded, exact solutions for d and k can be found by using a numerical method with fixed values of n, $\delta\Delta$, and Ψ values. Figure 7 shows k and d as a function of the refractive index n with $\delta\Delta_{dark} = 7.5°$ and $\Psi_{dark} = 5.22°$ (dotted line), and $\delta\Delta_{dom} = 18.3°$ and $\Psi_{dom} = 5.93°$ (solid line) for the mixed film.

The plots $d-n$ for dark and domain regions of the mixed TSPP/DOMA film (dotted and solid lines, respectively) can be overlapped by means of a factor of 2.86, i.e., $d_{dom} \approx 2.86 d_{dark}$ (circles in Figure 7) with a deviation less than 1%. Therefore, if n is almost constant, the thickness of the film at the bright domain must be approximately three times that for the dark regions (2.86). This result being independent of any proposed structural model of the film seems to confirm the previous hypothesis about the domain formation based on a trilayer structure.

On the other hand, the complex part of the refractive index, k, can be evaluated from the reflection spectroscopic data. The reflection can be related to the absorption and, in turn, to the imaginary part of the refractive index, k. In fact, the value of k is proportional to the absorbance, Abs, according to:

$$k = \frac{2.303 \cdot \lambda \cdot \mathrm{Abs}}{4\pi \cdot d} \qquad (7)$$

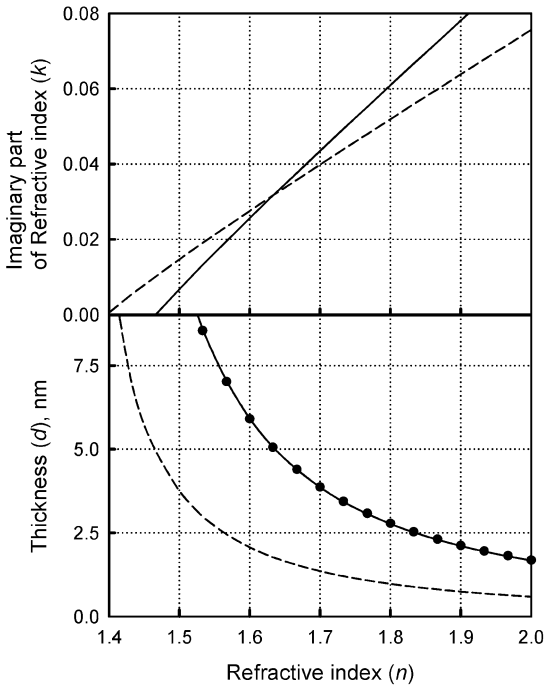

Figure 7. Plots of the theoretical *d* and *k* values versus *n* for the bright domains (solid line) and the dark region (dashed line) of the mixed monolayer. Dots on the solid line correspond to $2.86d_{\text{dark},0.8}$ for any *n* constant value.

where *d* is the sample path length and λ is the wavelength of the laser (532 nm). On the other hand, eq 1 can be written[25] as $\Delta R \approx 2.303 \cdot \text{Abs} \cdot (R_s)^{1/2}$. Combining this relation with eq 7 results in

$$\Delta R^{n} = \Delta R \cdot A = \frac{k \cdot d \cdot A \cdot 4\pi \cdot \sqrt{R_s}}{\lambda} \tag{8}$$

According to the normalized reflection spectra a constant value of ΔR^{n} is obtained at any surface density for $\lambda = 532$ nm (inset Figure 4). Therefore, and taking into account $d \cdot A \approx$ constant for bright and dark regions, then $k_{\text{dom}} \approx k_{\text{dark}}$. This condition is only satisfied for $n = 1.634$ (see Figure 7, top), being in this case $k = 0.0317$, $d_{\text{dark}} = 1.764$ nm, and $d_{\text{dom}} = 5.045$ nm (see Figure 7). The thickness values thus obtained are in good agreement with those estimated by molecular modeling. This fact shows that the estimation of the optical parameters, *n* and *d*, in the presence of absorption can be facilitated by using complementary techniques such as reflection spectroscopy.

Conclusions

The experimental results obtained from the $\pi-A$ isotherm, the reflection spectroscopy, BAM, and the ellipsometric analysis for the TSPP/DMPA = 1:4 film confirm that the observed collapse at high surface pressures ($\pi >$ 33.5 mN/m) corresponds to a phase transition between a monolayer and a trilayer with well-defined structure. For this high surface pressure the TSPP/DMPA = 1:4 film organizes into an ordered trilayer film at the air−water interface where a bilayer of DOMA molecules whose head polar groups retain the dimer porphyrins stands on top of the mixed monolayer where TSPP molecules are as a monomer (see Scheme 4).

By comparison with other similar systems such as anionic lipid/cationic water-soluble porphyrin,[21,22] it is noteworthy that although two ordered and reversible structures are obtained, the different molecular structure of the lipid matrix leads to a distinctive 3D array. The DMPA chains achieve a vertical orientation at high surface pressure, $A_{\text{chain}} = 0.20$ nm^2, acceding to all positive charges of the porphyrin molecules and consequently allowing the dimer formation underneath the monolayer matrix without such a matrix occupies additional area to that of the dimer. However, this is not possible for the TSPP/DOMA system due to the structure of DOMA molecule, short headgroup, and alkyl chains oriented slightly tilted. In this case, the lipid always contributes to the total area of the complex at the air−water interface. Thus, the dimer is surrounded laterally by DOMA molecules (see Scheme 3). We propose that when the density of those $\text{TSPP}_{\text{dimer}}$−DOMA complex increases, repulsions emerge, and the stability of the film decreases, so the collapse to a new 3D structure where the dimer is stable inside the lipidic bilayer (see Scheme 4) is facilitated.

Zhang et al.[28] did not detect the trilayer formation when the TSPP molecules were absorbed from the aqueous subphase to the DOMA monolayer formed at the air−water interface. Thus, they obtained complexes in which two DOMA molecules attached one TSPP molecule with an orientation tilted with respect to the interface and *J* aggregates were observed. This type of organization facilitates the formation of chiral aggregates.[28] Alternatively, the mixed TSPP/DOMA film described in this work was prepared at the air−water interface by cospreading and H aggregates were obtained. The mixed solution with a mixing ratio corresponding to the stoichiometry forms neutral monolayers pushing the complex formation of 1 TSPP molecule-4 DOMA molecules. This fact is crucial to explain the evolution of the collapse to a trilayer with a well-defined structure.

We have found a new system with a behavior not only similar to that observed for some thermotropic liquid crystals at the air−water interface,[4−6] but also reversible. This mixed film organizes by itself as a monolayer at low surface pressure and under compression avoiding a disarrangement structure leads to a highly ordered ultrathin films. This type of system could allow us under appropriate structural conditions to control and fabricate multilayers with a precise degree of arrangement at the air−water interface. The control of the structural parameters may open a new method to obtain a novel type of film at that interface.

Acknowledgment. The authors wish to express their gratitude to the spanish CICYT for financial support of this research in the framework of Project BQU2001-1792. Also, we thank the Ministerio de Ciencia y Tecnología for the contract of one of the authors (Ramón y Cajal Program).

Appendix

For isotropic film sandwiched between two isotropic media, the following coefficients are applied[26]

$$R_x = \frac{r_{01x} + r_{12x} e^{-i2\beta}}{1 + r_{01x} r_{12x} e^{-i2\beta}}$$

where r_{ijx} are the reflection coefficients at ambient-film ($i = 0$, $j = 1$) or film-substrate ($i = 1$, $j = 2$) for $x =$ p or s polarization, respectively.

$$r_{01p} = \frac{n_1^2 \cos(\varphi_0) - n_0\sqrt{n_1^2 - n_0^2 \sin^2(\varphi_0)}}{n_1^2 \cos(\varphi_0) + n_0\sqrt{n_1^2 - n_0^2 \sin^2(\varphi_0)}}$$

$$r_{12p} = \frac{-n_1^2 \cos(\varphi_2) + n_2\sqrt{n_1^2 - n_2^2 \sin^2(\varphi_2)}}{n_1^2 \cos(\varphi_2) + n_2\sqrt{n_1^2 - n_2^2 \sin^2(\varphi_2)}}$$

$$r_{01s} = \frac{n_0^2 \cos(\varphi_0) - \sqrt{n_1^2 - n_0^2 \sin^2(\varphi_0)}}{n_0^2 \cos(\varphi_0) + \sqrt{n_1^2 - n_0^2 \sin^2(\varphi_0)}}$$

$$r_{12s} = \frac{-n_2 \cos(\varphi_2) + \sqrt{n_1^2 - n_2^2 \sin^2(\varphi_2)}}{n_2 \cos(\varphi_2) + \sqrt{n_1^2 - n_2^2 \sin^2(\varphi_2)}}$$

where n_0, n_1, and n_2 are the refractive indexes of the ambient, film, and subphase, respectively. φ_0 and φ_2 are the angle of incidence and refraction on and from the subphase, respectively. They are related by the Snell law:

$$n_0 \sin(\varphi_0) = n_2 \sin(\varphi_2)$$

and

$$\beta = 2\pi(d_1/\lambda)\sqrt{n_1^2 - n_0^2 \sin^2(\varphi_0)}$$

where d_1 is the film thickness and λ is the wavelength of light. The ellipsometric ratio is

$$\rho = \left|\frac{R_p}{R_s}\right| = \tan(\psi)e^{i\Delta}$$

References and Notes

(1) Kaganer, V. M.; Möhwald, H.; Dutta, P. *Rev. Mod. Phys.* **1999**, *71*, 779.
(2) Kuhn, H. *Pure Appl. Chem.* **1965**, *11*, 345.
(3) Ries, H. E., Jr.; Swift, H. *Langmuir* **1987**, *3*, 853.
(4) Friedenberg, M. C.; Fuller, G. G.; Frank, C. W.; Robertson, C. R. *Langmuir* **1994**, *10*, 1251.
(5) Xue, J.; Jung, C. S.; Kim, M. W. *Phys. Rev. Lett.* **1992**, *69*, 474.
(6) de Mul, M. N. G.; Mann, J. A., Jr. *Langmuir* **1994**, *10*, 2311.
(7) Ferreira, M.; Dynarowicz-Latka, P.; Miñones, J., Jr.; Caetano, W.; Kita, K.; Schalke, M.; Lösche, M.; Oliveira, O. N., Jr. *J. Phys. Chem. B* **2002**, *106*, 10395.
(8) Gourier, C.; Knobler, C. M.; Daillant, J.; Chatenay, D. *Langmuir* **2002**, *18*, 9434.
(9) Huo, Q.; Russev, S. C.; Hasegawa, T.; Nishijo, J.; Umemura, J.; Puccetti, G.; Russell, K. C.; Leblanc, R. M. *J. Am. Chem. Soc.* **2000**, *122*, 7890.
(10) Hönig, D.; Möbius, D. *Thin Solid Films* **1992**, *210/211*, 64.
(11) Siegel, S.; Hönig, D.; Vollhardt, D.; Möbius, D. *J. Phys. Chem.* **1992**, *96*, 8157.
(12) de Mul, M. N. G.; Mann, J. A., Jr. *Langmuir* **1998**, *14*, 2455.
(13) Deng, J.; Polidan, J. T.; Farmer-Creely, C. E.; Viers, B. D.; Esker, A. R. *J. Am. Chem. Soc.* **2002**, *124*, 15194.
(14) Ries, H. E., Jr. *Nature* **1979**, *281*, 287.
(15) Birdi, K. S.; Vu, D. T. *Langmuir* **1994**, *10*, 623.
(16) Vollhardt, D.; Kato, K.; Kawano, M. *J. Phys. Chem.* **1996**, *100*, 4141.
(17) Ramos, S.; Castillo, R. *J. Chem. Phys.* **1999**, *110*, 7021.
(18) Fang, J.; Dennin, M.; Knobler, C.; Godovsky, Y. K.; Makarova, N. N.; Yokoyama, H. *J. Phys. Chem. B* **1997**, *101*, 3147.
(19) Buzin, A. I.; Godovsky, Y. K.; Makarova, N. N.; Fang, J.; Wang, X.; Knobler, C. M. *J. Phys. Chem. B* **1999**, *103*, 11372.
(20) Rapaport, H.; Kuzmemko, I.; Kjaer, K.; Howes, P. B.; Als-Nielsen, J.; Lahaz, M.; Leiserowitz, L. *Biophys. J.* **2001**, *81*, 2729.
(21) Martín, M. T.; Prieto, I.; Camacho, L.; Möbius, D. *Langmuir* **1996**, *12*, 6554.
(22) Pedrosa, J. M.; Pérez, M.; Prieto, I.; Martín, M. T.; Möbius, D.; Camacho, L. *Phys. Chem. Chem. Phys.* **2002**, *4*, 2329.
(23) Hada, H.; Hanawa, R.; Haraguchi, A.; Jonezawa, Y. *J. Phys. Chem.* **1985**, *89*, 560.
(24) Martín, M. T.; Möbius, D. *Thin Solid Films* **1996**, *284−285*, 663.
(25) Grüniger, H.; Möbius, D.; Meyer, H. *J. Chem. Phys.* **1983**, *79*, 3701.
(26) Azzam, R. M. A.; Bashara, N. M. *Ellipsometry and Polarized Light*; Elsevier Science B. V.: Amsterdam, The Netherlands, 1999.
(27) Gaines, G. L. J. *Insoluble Monolayers at Liquid−Gas Interfaces*; Wiley-Interscience: New York, 1966.
(28) Zhang, L.; Lu, Q.; Liu, M. *J. Phys. Chem. B* **2003**, *107*, 2565.
(29) Drude, P. *Wiedemanns Ann. Physik* **1889**, *39*, 532.
(30) Drude, P. *Wiedemanns Ann. Physik* **1889**, *39*, 865.
(31) Tsukruk, V. V. *Prog. Polym. Sci.* **1997**, *22*, 247.
(32) Czikkely, V.; Försterling, H. D.; Kuhn, H. *Chem. Phys. Lett.* **1970**, *6*, 207.
(33) Grüniger, H.; Möbius, D.; Lehmann, U.; Meyer, H. *J. Chem. Phys.* **1986**, *85*, 4966.
(34) Pedrosa, J. M.; Dooling, C. M.; Richardson, T. H.; Hyde, R. K.; Hunter, C. A.; Martin, M. T.; Camacho, L. *Langmuir* **2002**, *18*, 7594.
(35) Kuhn, H.; Försterling, H. D. *Principles of Physical Chemistry*; John Wiley & Sons: New York, 1999.
(36) Pedrosa, J. M.; Martín-Romero, M. T.; Camacho, L.; Möbius, D. *J. Phys. Chem. B* **2002**, *106*, 2583.
(37) Prieto, I.; Martín-Romero, M. T.; Camacho, L.; Möbius, D. *Langmuir* **1998**, *14*, 4175.